Volume 24, No 1 | International Journal of Radiation Research, January 2026

# Differentiation of metastatic and primary brain tumor using magnetic resonance imaging

**M. Yasir[1], F. Siddique[2], F. Andleeb[3,4], G. Gilanie[5], H. Ullah[1*]**

[1]*Biophotonic Imaging Techniques Laboratory, Institute of Physics, The Islamia University of Bahawalpur, Bahawalpur, Pakistan*
[2]*Department of Physics, Lahore Garrison University, Sector C, DHA Phase 6, Lahore, Pakistan*
[3]*Department of Physics, Govt Sadiq Women University of Bahawalpur, Pakistan*
[4]*Walsh Lab, Biomedical Engineering department, Texas A and M university. College Station, Texas, USA*
[5]*Department of Artificial Intelligence, Faculty of Computing, The Islamia University of Bahawalpur, Bahawalpur, Pakistan*

► ***Original article***

***Corresponding author:***
*Janjua, Hafeez Ullah, M.D.*
***E-mail:*** *hafeezullah@iub.edu.pk*

**Received:** November 2024
**Final revised:** June 2025
**Accepted:** August 2025

***Int. J. Radiat. Res., January 2026; 24(1): 259-265***

**DOI:** 10.61186/ijrr.24.1.38

***Keywords:*** *Primary brain tumors, metastatic brain tumors, MRI, semi-automated segmentation, computer-assisted image interpretation.*

## ABSTRACT

***Background:*** Brain tumor segmentation is an important aspect of medical image processing. Timely detection of brain tumors can increase a patient's survival rate significantly. Doctors use traditional manual techniques for diagnosis, but these techniques are tedious and require intricate programming. ***Materials and Methods:*** New developments of automatic and semi-automatic approaches for image processing have been applied. MRI images are characterized using segmentation and registration Toolkit (ITK-SNAP) software to find and demarcate boundaries and assess brain tumor volume from MRI images. This study included six untreated brain tumor patients (aged 35-75) to explore the feasibility of using semi-automated MRI techniques for tumor segmentation. Despite the small sample size, the method showed promising accuracy, highlighting its potential for clinical use. ***Results:*** Our findings revealed accurate diagnosis of primary brain tumors, 3D tumor size, tumor edges, and metastatic brain tumors based on MRI images. ITK-SNAP proved to be more effective for diagnosing metastatic and secondary brain tumors than conventional techniques. The importance of effective and accurate segmentation, particularly discrimination among primary and metastatic tumors, was highlighted. ***Conclusion:*** On the contrary, completely automatic approaches tend to be imprecise. Tailoring the ITK-SNAP tool for brain tumor segmentation maximizes efficiency with improved accuracy for differentiating tumor categories.

## INTRODUCTION

Brain tumors possess a wide range of complex groups of abnormalities, categorized into two main types: primary and secondary (metastatic). Primary brain tumors have their origin from within the brain tissue itself, while metastatic tumors originate elsewhere in the body and spread to the brain, presenting therapeutic challenges [1]. Detecting and accurately assigning these tumors is vital for proper treatment planning. However, the task is largely difficult due to the inconsistent shapes and sizes the tumors assume, and also where the tumors are in the brain [2, 3].

The major causes of abnormal cells in the human body are poison intake, radiation exposure, trauma (severe injury inside the body), and viral attacks. There are collectively six types of brain tumors on the basis of grading, which are medulloblastoma, meningioma, lymphoma, glioma, pituitary adenoma, and craniopharyngioma [4, 5]. Benign and malignant are the major types of brain tumors, which are classified based on uncontrolled growth of a mass developed by an unwanted cell. It may present in different parts of the brain, such as the blood vessels, the cerebrum, the lymphatic tissue, the skull, and the pituitary glands [6]. Brain tumors also affect the surrounding tissue because they have no clear or stationary boundary, which distorts the neighboring tissue. Malignant is the dangerous stage of cancer that grows within brain tissue, with a low survival rate. Brain tumors directly affect the nervous system of the human body. Headache, shortage of sleep, body parts not working properly, nausea, memory loss, and smell loss are the major symptoms of brain tumors [7, 8].

Medical imaging is a very promising method for the diagnosis of brain tumors. These techniques include magnetic resonance imaging (MRI) [9], X-radiation (X-ray), Computed Tomography (CT), and Positron Emission Tomography (PET). MRI and Computer tomography are reliable techniques for the detection and visualization of cancer. Traditional segmentation techniques, which are widely in use, are labor-intensive, extremely time-consuming, and highly susceptible to human error, particularly when



[ DOI: 10.61186/ijrr.24.1.38 ]

dealing with significantly complex and irregular boundaries of tumors [10]. Fully automated approaches to segmentation, driven by artificial intelligence (AI), are fast and efficient but struggle to achieve the precision needed for accurate boundary detection for the tumor. Semi-automated methods provide a balanced alternative, combining user guidance with automated processes to streamline segmentation while preserving a high degree of accuracy [11].

Magnetic Resonance Imaging (MRI) is a stellar imaging modality and a preferred diagnostic tool because of its superior resolution, making it particularly advantageous in distinguishing between various types of brain tissues. However, despite its (MRI) excellent contrast capabilities on soft tissues, it falls short of the high (spatial) resolution needed for finer details [12]. In this study, we use MRI's strengths in contrast enhancement and leverage on a semi-automated segmentation tool, ITK, enhanced with critical adaptations to improve the outcomes for brain tumors.

It also gives high-resolution images with non-invasive characteristics and works on the principle of nuclear magnetic resonance. Along with good medical imaging, the process of segmentation is very important for image analysis in the biomedical field. A fully automated method based on Gaussian model mixture has been used in the past. This technique contains multi-level fusion and a model of a reshaping method. This technique is difficult to operate due to the involvement of adjacent neighboring tissues, which may affect the desired part of the segmentation [13]. Therefore, fully automatic segmentation approaches can cause errors in the evaluation of the infected part of the body or tissue and consequently can affect the results. While comparing automatic techniques with manual segmentation, the manual technique totally relies on human methodologies, and the segmentation process is very slow. Manual is impractical as well due to the complex fusion of data in the shearing volume problem in tissue [14]. The approach of semi-automated segmentation requires human and computer involvement and has a powerful algorithm. It is a very effective and practical tool for image processing that provides information about the infected area and helps in diagnosing the exact location of the tumor in the human body. Among many other semi-automated software, ITK-Snaps is a very effective tool for visualization and segmentation of MRI images. It was designed in the early 2000s, is easy to access for every person under control, and does not require any programming for segmentation [15]. Paula Martins *et al.* worked with the manual segmentation by using ITK snaps, which was considerably more productive than manual division. They altogether reduced the time (from 30 to 6 minutes) and divided activities, which is appropriate within the scope of a broad database. In the work presented here, we used the algorithm operated by the imaging software ITK snaps for MRI brain image segmentation. This work focuses on feature extraction and validation of finding the infected tissue in the brain, i.e., properties showing that the algorithm is close to the K-means. Also used the fuzzy k-means algorithm for the automatic segmentation of brain images for the detection of the tumor tissue in the human brain, but the ITK snaps technique. This work also highlighted and colored segmentation by using the ITK snap properties to check the intensity and tendency of brain tumors [16].

This study introduces a novel approach to brain tumor segmentation by leveraging the semi-automated ITK-SNAP software, specifically customized for identifying and differentiating primary and metastatic tumors. While traditional manual methods are accurate, they are labor-intensive and prone to errors. Fully automated methods often lack precision, especially when dealing with complex tumor boundaries. By combining the strengths of both manual and automated techniques, our approach provides a more efficient, accurate, and user-friendly solution for brain tumor diagnosis. This study emphasizes the critical need for precise segmentation to improve clinical outcomes, highlighting the potential of ITK-SNAP as an invaluable tool in neuro-oncology diagnostics.

## MATERIALS AND METHODS

### *Dataset and algorithm*

This study has utilized the MRI data obtained from a group of patients who have both cases of primary as well as metastatic tumors. The data set has MRI scans and also details the consequences. The data from all patients were made anonymous to prevent breach of their privacy. We have utilized two standards of databases. One database was gathered from master radiologists, which included images of cancer patients with cuts for every patient and others for sampling.

### *Case study*

This study involved six patients with brain tumors, aged 35 to 75 years (mean age: 55 years). The group consisted of 3 male and three female patients. All patients were diagnosed with either primary brain tumors (e.g., gliomas, meningiomas) or metastatic brain tumors originating from other body parts. Patients were selected from the Radiology Department of Sheikh Zaid Hospital, Rahim Yar Khan, Pakistan, and had not undergone any prior medical treatment for their tumors. All patient data were anonymized in compliance with privacy regulations.

The small sample size of 6 patients in this study is justified for several reasons. As a pilot study, it



[ DOI: 10.61186/ijrr.24.1.38 ]

focuses on testing the feasibility and effectiveness of semi-automated MRI tumor segmentation using ITK-SNAP. The results, including high diagnostic accuracy and AUC values, provide strong evidence of the method's potential despite the limited sample. Moreover, due to the exploratory nature of this study, the small sample is adequate for initial data collection, with plans for larger cohorts in future research to validate and expand upon these findings.

Test images of 6 brain tumor patients were collected from the hospital and in the extension of DICOM. Calculation is invariant to interpretation, and additionally, coefficients do not change regardless of the sign being moved. A programming algorithm identifies the tumor MRI image and differentiates the ordinary and irregular tissues in brain images. We are using software such as Onis from Germany and ITK -SNAP (USA) for different properties of brain tissue [17].

***Mechanism of segmentation***

MRI imaging was performed using a 3 Tesla MRI system (Siemens Magnetom, Germany), which offers high spatial resolution essential for accurate brain tumor analysis. Patients were positioned in the scanner, and typical imaging sequences included T1-weighted, T2-weighted, and FLAIR to differentiate between tumor tissue and surrounding brain structures. Contrast-enhanced imaging using gadolinium-based agents (Gadavist, USA) was performed to improve tumor visibility. The scans were acquired with a voxel size of 1-2 mm for detailed tumor boundaries. Data from these scans were processed using ITK-SNAP software for semi-automated segmentation and tumor analysis.

The process of segmentation for modalities of multiple MRI images is used to develop the speed image, which is scalar and ranges from -1 to 1, as given in equation 1.

$$g(x) = P(x \in S) - P(x \in \Omega \setminus S) \quad (1)$$

Where; S is the structure of the foreground, Ω is the domain of the image classifier providing the features to apply to every voxel in the domain of the MRI image. Resulting probabilities $P^k(x)$ for every voxel $x$ and every class k, joined to develop the structure of the interested part of the tissue, are given in equation 2;

$$\partial C/\partial t = [g(C) + \alpha\kappa C]\, NC \quad (2)$$

Where; C represents the boundary of the segmented region, κC shows the mean curvatures. NC indicates the unit of C from outside the tissue, and α is the parameter of scale. In the process of evaluating the infected part, the contour is stretched into the areas where g(x) is positive and shrinks when g(x) is negative. Hence, the curvature parameter α supplies the smoothness of C. probabilities are given by equation 3;

$$P(x \in S) > P(x \in \Omega \setminus S) \quad (3)$$

Resulting contour C provides the visualization of 3D slices in real time and allows the user to stop the process of evaluation at any time. The average time for segmentation is approximately the first data set. 11.7 ± 4.2 minutes for 1st rater and 1st attempt, while 10.4 ± 5.5 minutes for 1st rater 2nd attempt, lastly 4.8 ± 9.7 minutes for 2nd rater. Each pixel (or voxel) in an image can be said to be one hub in the grid P. Let $xi$ tells to a power estimation of a solitary pixel (or voxel) with a position $i$ in a picture $\vec{x} = (x\ 1...m)$ characterized over a limited cross section P, where $m$ is the all-out number of picture components ($m = MN$ for a 2D image and $m = MND$ for a 3D image). Let N signify a neighboring framework for a grid of P, where N$i$ is a little neighborhood around $i$, excluding $xi$. The hubs (pixels/voxels) in a cross-section pair are identified with each other by means of a neighborhood framework N that can be characterized as given in equation 4;

$$N = (N i \mid \forall i \in P) \quad (4)$$

## RESULTS

***Segmentation through image processing***

Figure 1 illustrates the segmentation process of a brain tumor from DICOM (OsiriX, USA) MRI images using image processing techniques. It begins with the original MRI scans (A–C), followed by intensity adjustments and filtering (D–F), and ends with tumor segmentation results (G–H), showing the localized affected area. This step-by-step method supports accurate identification and 3D modeling of the brain tumor for clinical analysis.

DICOM image was selected with the tumor for the segmentation, which shows the abnormal part of the brain as shown in figure 2. Figure 2 (A-D) shows the segmentation of white and grey matter in MRI images using ITK-SNAP. The clear boundaries of each tissue type are highlighted, aiding in the precise identification of brain structures

Figure 3 represents the white or grey matter visible with a clear boundary in software interference. The datasets portioned with this segment introduces the aftereffects of our proposed image division method and Voxel/pixel size differences contingent upon imaging parameters such as magnet quality time. Usually, the voxel size in MRI studies is of the order of 1-2 mm. Evaluation of the infected part in the MRI image through segmentation and ITK snaps helps to generate the 3D model of localized tumor in the brain, as shown in the C portion of the interface. As shown in figure 4, ITK snaps are used to implement semi-automatic segmentation, which is based on region boundary



[ DOI: 10.61186/ijrr.24.1.38 ]

selection (region competition snakes). There are some important steps for segmentation of the brain, comprising: selecting the region of the infected part of the brain, resampling of the MRI image for isotropic voxels, describing a threshold value for clustering, placing bubble snakes inside the tumor, and contour control evaluation, which gives a 3D model of the brain tumor through the algorithm.

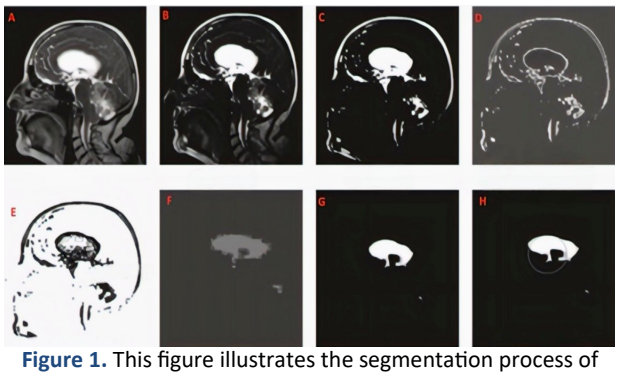

**Figure 1.** This figure illustrates the segmentation process of brain tumors in MRI images using ITK-SNAP. **(A)** Original MRI scan, **(B)** tumor region highlighted, **(C)** skull-stripped image, **(D)** edge extraction, **(E)** decomposed image, **(F)** clear tumor boundaries, **(G, H)** final. Segmentation. The process clearly defines the tumor area, enabling accurate analysis and measurement for diagnosis.

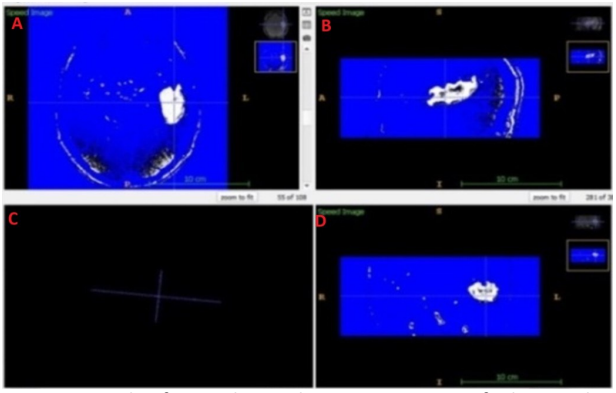

**Figure 2.** This figure shows the segmentation of white and grey matter in MRI images using ITK-SNAP. The clear boundaries of each tissue type are highlighted, aiding in the precise identification of brain structures (**A, B, C** and **D**).

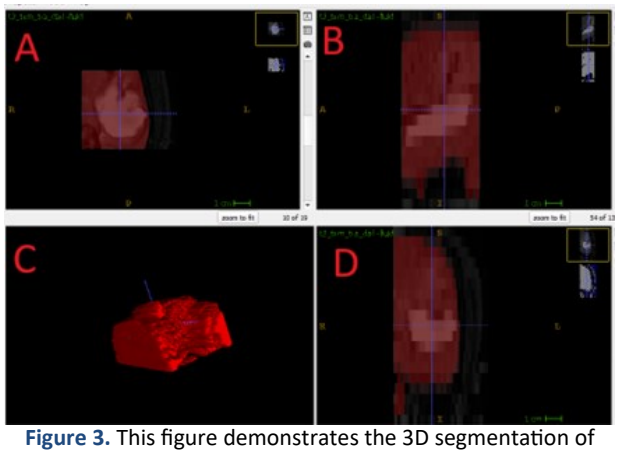

**Figure 3.** This figure demonstrates the 3D segmentation of brain tumors using ITK-SNAP. **(A)** Irregular tumor boundary, **(B)** extracted MRI image, **(C)** 3D tumor model, **(D)** clustering of segmented tumor area. The process visualizes tumor volume and shape effectively.

In figure 4, raw images are extracted to enhance their pixel quality through a contrast label, which separates the infected tissue from its background. Active contour develops the decomposed MRI image to describe the actual tumor boundary and shape. By virtue of a head MRI, image segments are customarily requested into three major tissue types: white matter (WM), gray matter (GM), and cerebrospinal fluid (CSF) [18].

Here, we segmented some brain tumor images with metastases in the brain tumor using this process. We can easily visualize and diagnose this type of brain cancer. Some of our patients have metastatic brain tumors that are highlighted in the images given below, which were run with the segmented process through the MR images. The malignant brain tumor diagnosis in neural network deep inside the brain, shown in figure 6, rotates the 360-degree angle with the help of software and elaborates every angle of grey matter movement in a rotation cycle, which helps to diagnose and study the abnormalities of brain tumors through voxels. As shown in Figure 6, the tumor is present in the neural structure of the brain, and through the DICOM image analysis, we can see that the 360-degree rotation of the tumor helps to understand its size and actual location. An atlas-based method used for the segmentation of tumors with vessels of the whole head develops the structural information. The atlas splits a magnitude of MRI images into numerous vascular boundaries; each of them has definite vascular properties. It can be functional to the magnitude of the MRI image of the entire head by distorted matching, which helps in the segmentation of blood vessels from the connected phase image. This algorithm forms the arterial and venous trees through iteratively adding voxels that are selected based on their gray scale value and changes in values in their neighborhood vessels.

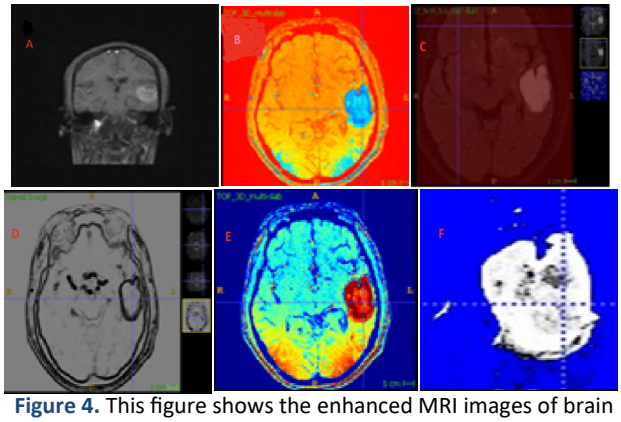

**Figure 4.** This figure shows the enhanced MRI images of brain tumors. **(a)** Original MRI image, **(b)** contrast-enhanced MRI, **(c)** skull-exposed MRI, **(d)** edge extraction, **(e)** decomposed image, **(f)** clear tumor boundaries. The process highlights the tumor area, enhancing visibility and accuracy for segmentation and diagnosis.

The procedure of MR segmentation is similar to normal tumor segmentation, operating with ITK



[ DOI: 10.61186/ijrr.24.1.38 ]

snaps, which provides the most effective method to visualize and segment the MR images. The metastatic brain tumors are delocalized and affect the tissue of the brain, or any part of the brain, which is severe and dangerous to the health of the patient. Because the secondary type of brain tumor is very injurious and has a minimal chance of survival, if the patient is not treated properly on time, the tumor location may be fatal. ITK snaps provide the facility of enhanced image by contrast setting and show the boundary of the tumor very clearly. After the semi-automatic segmentation, we are able to see the exact location, size, and boundary of the metastatic brain tumor (see figure 6). The total time of the semi-automatic segmentation ranges approximately -6 to 7 minutes.

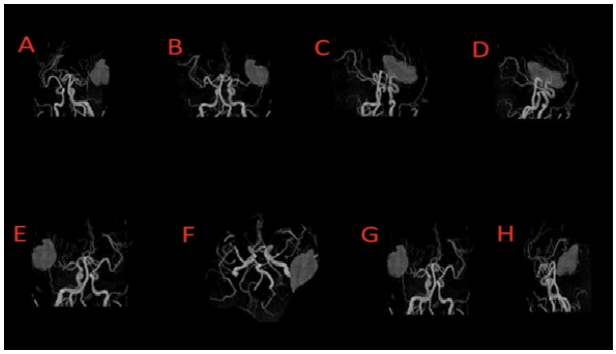


**Figure 5.** This figure shows the 360-degree rotation of a brain tumor using MRI images. The rotation helps visualize the tumor's size, shape, and location, aiding in precise diagnostic evaluation through voxel analysis (**A, B, C, D, E, F, G,** and **H**).

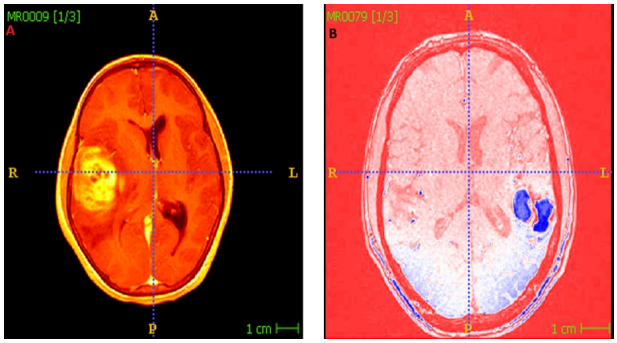


**Figure 6. (a)** Contrast-enhanced MRI image highlighting the brain tumor region, **(b)** Segmented image showing the clear boundaries of a metastatic brain tumor. This demonstrates enhanced tumor visualization and precise segmentation for accurate diagnosis.

The tumor is reviewed into four distinct evaluations from evaluation 1 to evaluation 4, depending on the size, forcefulness, and power of the tumor. From the above images, the segmented metastases in the brain tumor clearly show that they are delocalized in the brain. A network of bubbles snakes to create the detailed segmented image that provides the qualitative 3D evaluation, including position, overall brain configuration, existence, and location of the tumor. These images are extracted with the help of the ITK snaps, which is very helpful for the segmentation of MR images [19].

Table 1 shows different features, "pixel value, mean, standard deviation, areas of infected tissue, and RMS value," that differentiate the normal and metastatic brain tumors. These properties are obtained using the ITK snaps and Onis software. A t-test comparing the tumor areas of primary and metastatic brain tumors showed a statistically significant difference ($t(10) = 2.98$, $p=0.045$). Metastatic tumors demonstrated larger mean tumor areas compared to primary tumors. This finding supports the effectiveness of the semi-automated ITK -SNAP segmentation method in distinguishing tumor types based on size and volume.

**Table 1.** Different feature pixel values, mean, standard deviation, areas of infected tissue, and RMS (Root Mean Square) value differentiate the normal and metastatic brain tumors.

| Patient No. | Images | Pixel Value | Mean | Standard Deviation | Area ($cm^2$) | RMS |
|---|---|---|---|---|---|---|
| 1 | 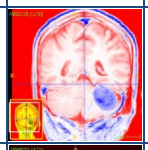 | 834 | 781.29 | 109.55 | 16.007 | 0.089971 |
| 2 | 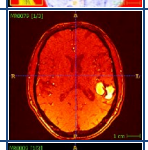 | 703 | 633.56 | 124.96 | 10.529 | 0.089027 |
| 3 | 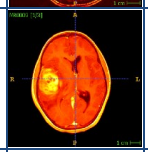 | 792 | 703.05 | 143.71 | 13.610 | 0.088943 |
| 4 | 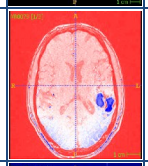 | 677 | 569.34 | 102.56 | 11.439 | 0.089278 |
| 5 | 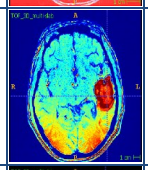 | 943 | 684.47 | 123.60 | 12.447 | 0.089564 |
| 6 | 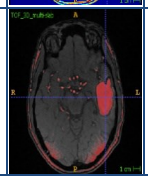 | 890 | 680.51 | 122.43 | 12.104 | 0.089137 |

## DISCUSSION

The main finding of this research/study has been that a semi-automated or customized approach to MRI has a considerable level of reliability, accuracy, and efficiency. In this study, six patients with brain tumors were examined, and statistical comparisons were made between the patient groups. MRI images, pixel values, statistical results, and medical information for each patient are accurate and presented in table 1. The results were similar across



[ DOI: 10.61186/ijrr.24.1.38 ]

all patients, and no statistically significant differences were found between them. For the segmentation of tumor images, the semi-automated algorithm of ITK snaps is used. The image processing technique differentiates between normal brain tumors and metastatic brain tumors, showing the tendency of infected tissue in the human brain. If the value is less than the central tendency, it is said to be a normal or primary brain tumor. However, if the value is greater than the central tendency, then it is said to be a metastasis or secondary brain tumor. Our results are based on the segmentation of brain tumors in which we set the algorithm of ITK snaps to build the 3D model of the tumor. There are four important steps for segmentation of brain tumor through ITK snaps including (i) selecting the region of infected part of brain, (ii) resampling of MRI image for isotropic voxels, (iii) describing threshold value for clustering, and (iv) placing bubble snakes inside the tumor and contour control evaluation gives 3D model of brain tumor through the algorithm. ITK snaps and Onis give parameters such as pixel value, mean, standard deviation, area covered by the tumor, and the root mean square value of the brain tumor.

Our work is nearly relevant to the research work by Gumus *et al*. [20] but they used the algorithm operated by MATLAB for segmentation. Feature extraction and validation of infected tissue in the brain also resembles this work, as the extracted properties in both algorithms are very close to the K-means [21]. The fuzzy k-means algorithm was also used for the automatic segmentation of brain images to detect tumor tissue in the human brain [16]. The segmented part of brain images using the computer algorithm gives a colored visualization of infected tissue. Our work also gives several parameters, such as highlighted or colored segmentation, intensity, and the tendency of brain tumors. Martins *et al*. [24] worked using ITK snaps, and they found it considerably more productive than manual division, along with reduced time (from 30 to 6 minutes) and division activities [25-26]. Our technique is similar to the one(1) because they also used the software ITK snaps for segmentation of MR images.

This research has a number of limitations, which need to be taken into account when analyzing the findings. The sample population of six patients is relatively small, which confines generalizability. A greater sample size would yield stronger data and greater statistical power for analysis. Furthermore, using MRI data from a solitary source involves potential sources of bias, including undiagnosed defects within a given scanner, which would impact image quality and also affect accuracy of segmentation [27]. Finally, though ITK-SNAP is a versatile tool, the use of semi-automatic input makes it vulnerable to human error or subjective interpretation, which would affect overall accuracy.

## CONCLUSION

This study has successfully demonstrated to a great extent how reliable a semi-automated segmentation is. When fully customized, it provides a significantly powerful and practical solution for the MRI-based differentiation of brain tumors. An Adjusted ITK snap workflow is able to achieve very efficient and accurate segmentation that distinguishes the primary and metastatic tumors. This groundbreaking achievement of this study potentially raises the standards of clinical diagnosis and accompanying workflows in the field of neuro-oncology. This research is precise and highly valuable in enhancing diagnostic accuracy in the medical field. Semi-automated segmentation techniques are more promising than traditional manual and fully automated techniques. We have found that Semi-automated software ITK snaps and Onis have the potential to process MRI images to diagnose primary and metastatic brain tumors. Further research on this area in the future can apply this approach and study other forms of tumors and relevant imaging modalities. This will further broaden its applicability in clinical medicine.

***Ethical committee approval*:** Ethical Approval for this study was obtained from the Institutional Review Board of the Radiology Department, Sheikh Zayed Hospital, Rahim Yar Khan, Pakistan. The study was registered under protocol number SZH/ IRB/2021/015, with approval granted on March 15, 2021, ensuring compliance with ethical research standards.

***Competing interest*:** The authors have no relevant financial or non-financial interests and competing interest to disclose.

***Data availability*:** The authors confirm that the data supporting the findings of this study are available within the article.

***Authors' contribution*:** M.Y.: Conceptualization, experimentations, original drafting; F.S.: Data collection; F.A.: Review of analysis; G.G.: Software, Conceptual review and analysis; H.U.: Supervision, Visualization, resources.

***AI usage*:** Not AI was used for manuscript write-up.

## REFERENCES

1. Khan Z, Yahya N, Alsaih K, Al-Hiyali MI, Meriaudeau F (2021) Recent automatic segmentation algorithms of MRI prostate regions: a review. *IEEE Access, **9**: 97878-905*.
2. Panic J, Defeudis A, Mazzetti S, Rosati S, Giannetto G, Vassallo L, *et al.*, editors. A Convolutional Neural Network based system for Colorectal cancer segmentation on MRI images. 2020 42nd Annual International Conference of the IEEE Engineering in Medicine & Biology Society (EMBC); 2020: IEEE.
3. Ebrahimi A, Khoramian D, Tabatabaei N, Sarvizadeh S (2024) Temozolomide overdose in treating high-grade glioma: A case report. *International Journal of Radiation Research, **22**(3): 807-9*.
4. Sun Z, Wu P, Cui Y, Liu X, Wang K, Gao G, *et al.* (2023) Deep-



[ DOI: 10.61186/ijrr.24.1.38 ]

learning models for detection and localization of visible clinically significant prostate cancer on multi-parametric MRI. *Journal of Magnetic Resonance Imaging,* ***58****(4): 1067-81*.
5. Muhammad AP, Harto AW, Sardjono Y, Wijaya GS, Ismail Z, Triatmok IM, *et al.* (2023) Dose and irradiation time analysis of negative pi-meson therapy using particle and heavy ion transport code system (PHITS). *International Journal of Radiation Research,* ***21****(4): 653-61*.
6. Schelb P, Wang X, Radtke JP, Wiesenfarth M, Kickingereder P, Stenzinger A, *et al.* (2021) Simulated clinical deployment of fully automatic deep learning for clinical prostate MRI assessment. *European Radiology,* ***31****: 302-13*.
7. Mark BWLH. and Mengel SA (2002) Chapter 10 in Fundamentals of clinical practice," in making a diagnosis. SBN 0-306-46692-9, 2002; pp: 197-198..
8. Shan J, Wen Y, Guo Y (2025) Clinical analysis of gamma knife radiosurgery for pituitary adenomas. *International Journal of Radiation Research,* ***23****(1): 61-8*.
9. Zhang L and Sun M (2024) The Application of 3.0 T magnetic resonance perfusion-weighted imaging in the differentiation and grading of brain gliomas. *International Journal of Radiation Research,* ***22****(3): 573-8*.
10. Tsehay YK, Lay NS, Roth HR, Wang X, Kwak JT, Turkbey BI, *et al.*, editors. Convolutional neural network based deep-learning architecture for prostate cancer detection on multiparametric magnetic resonance images. Medical imaging 2017: Computer-aided diagnosis; 2017: SPIE.
11. Arif M, Schoots IG, Castillo Tovar J, Bangma CH, Krestin GP, Roobol MJ, *et al.* (2020) Clinically significant prostate cancer detection and segmentation in low-risk patients using a convolutional neural network on multi-parametric MRI. *European Radiology,* ***30****: 6582-92*.
12. Schweitzer T, Vince G, Herbold C, Roosen K, Tonn J-C (2001) Extraneural metastases of primary brain tumors. *Journal of Neuro-Oncology,* ***53****: 107-14*.
13. Fink KR and Fink JR (2013) Imaging of brain metastases. *Surg Neurol Int,* ***4****(Suppl 4): S209*.
14. Kouli O, Hassane A, Badran D, Kouli T, Hossain-Ibrahim K, Steele JD (2022) Automated brain tumor identification using magnetic resonance imaging: A systematic review and meta-analysis. *Neuro-Oncology Advances,* ***4****(1): vdac081*.
15. Cuellar-Baena S, Morais L, Cendes F, Faria AV, Castellano G (2011) Manual and semi-automatic quantification of in vivo $^{1}$H-MRS data for the classification of human primary brain tumors. *Brazilian Journal of Medical and Biological Research,* ***44****: 345-53*.
16. Ganesh M, Naresh M, Arvind C (2017) MRI brain image segmentation using enhanced adaptive fuzzy k-means algorithm. *Intelligent Automation & Soft Computing,* ***23****(2): 325-30*.
17. Joseph RP, Singh CS, Manikandan M (2014) Brain tumor mri image segmentation and detection in image processing. *Int J Res Eng Technol,* ***3****(1): 1-5*.
18. Rajan S (1998) MRI Hardware System Components. pp. 25-39.
19. Zaman A, Ullah K, Ullah R, Imtiaz H, Yu D (2019) Image segmentation of mri image for brain tumor detection. *Int J Eng Appl Sci Technol,* ***04****: 50-5*.
20. Gumus KZ, Menendez M, Baerga CG, Harmon I, Kumar S, Mete M, *et al.* (2025) Investigation of radiomic features on MRI images to identify extraprostatic extension in prostate cancer. *Computer Methods and Programs in Biomedicine,* ***259****: 108528*.
21. Calimano-Ramirez LF, Virarkar MK, Hernandez M, Ozdemir S, Kumar S, Gopireddy DR, *et al.* (2023) MRI-based nomograms and radiomics in presurgical prediction of extraprostatic extension in prostate cancer: a systematic review. *Abdominal Radiology,* ***48****(7): 2379-400*.
22. Yazdani S, Yusof R, Karimian A, Pashna M, Hematian A (2015) Image segmentation methods and applications in mri brain images. *IETE Technical Review,* ***32****(6): 413-27*.
23. Dhiman A and Satpute P (2019) Brain tumor segmentation in MRI images. *Int J Res Adv Technol,* ***7****: 10-4*.
24. Martins P, Oliveira C, Silva S, Silva A, Teixeira A (2011) Tongue segmentation from MRI images using ITK-SNAP: Preliminary Evaluation. In: International Conference Computer Graphics, Visualization, Computer Vision and Image Processing. July, Rome, Italy, 2011, pp 3–10.
25. Martel-Pelletier J, Paiement P, Pelletier J-P (2023) Magnetic resonance imaging assessments for knee segmentation and their use in combination with machine/deep learning as predictors of early osteoarthritis diagnosis and prognosis. *Therapeutic Advances in Musculoskeletal Disease,* ***15****: 1759720X231165560*.
26. Gholamiankhah F, Mostafapour S, Arabi H (2022) Deep learning-based synthetic CT generation from MR images: comparison of generative adversarial and residual neural networks. *International Journal of Radiation Research,* ***20****(1): 121-30*.
27. Bliznakova K, Georgiev T, Sarno A, Teneva T, Dukov N, Okkalidis N, *et al.* (2024) A comparison of two low-cost 3D printing techniques for constructing phantoms from MRI breast images. *International Journal of Radiation Research,* ***22****(4): 883-90*.



[ DOI: 10.61186/ijrr.24.1.38 ]